MODELLING SHEET-FLOW OF MASSIVE PARTICLES USING A TWO-PHASE APPROACH BASED ON A FRICTIONAL RHEOLOGY.

Thibaud Revil-Baudard[1], Julien Chauchat[2]

Abstract

In this paper, a two-phase model is presented to describe the sheet flow regime of sediment transport. A $\mu(I)$ rheology and a mixing length approach are used for intergranular stresses and turbulent stresses modelling respectively. In the model two layers are considered, a dilute suspension layer and a dense sediment bed layer. The concentration profile is obtained from the granular dilatancy law $\phi(I)$ in the sediment bed layer and from a Rouse profile in the suspension layer. The results obtained by the present model show a good agreement with experimental data in terms of velocity and concentration profiles and solid load. In particular, the model seems to be able to fairly describe the transition from the dense static bed up to the dilute suspension. It demonstrates that the dense granular rheology is relevant to describe intense bed-load transport in turbulent regime (sheet flow).

Key words : Sediment transport, Sheet flow, Two-phase flow, Frictional rheology, turbulence.

1. Introduction

The sheet flow regime of sediment transport is linked to extreme events such as sand storms, river floods or storm waves in the surf zone. Because of the huge amount of sediment transported in this regime it is especially important for the understanding of the morphological evolution and the stability of constructions in riverine and coastal environments. The sheet flow regime is characterized by a high Shields number θ, ratio of the force exerted by the fluid on the sediment bed over the apparent weight of a single particle. It is usually considered that sheet flow occurs for Shields number higher than 0.5. In sheet flow regime, the sediment bed is flat, and the thickness of the bed-load layer δ_s is of order of several times the particle's size d_p. It is widely accepted that particle-particle interactions, such as collisions and frictional interactions, and fluid turbulent velocity fluctuations are the key mechanisms controlling the sheet flow (Bagnold, 1954; Hanes and Bowen, 1985 amongst others). First attempts in modelling sheet flow have been proposed by Hanes and Bowen (1985) or Wilson (1987), amongst others. In these models the concentration profile is prescribed and the intergranular stresses are given by a phenomenological law (e.g. Bagnold, 1954). Over the past fifteen years, two-phase models, based on kinetic theory of granular flows to describe intergranular stresses, has been applied with some success to model the sheet flow regime (e.g. Jenkins and Hanes, 1998 ; Hsu et al., 2004). In these models, the kinetic theory has been stated for situations in which collisional interactions are the dominant mechanism of momentum transfer. The concentration profile is obtained from a balance between collisional interactions and gravity as a result of the model. Recent improvements in the understanding of the liquid regime of dense granular flows (GDR midi, 2004; Cassar et al., 2005; Forterre and Pouliquen, 2008; Boyer et al., 2011) has led to the $\mu(I)/\phi(I)$ rheology. This rheology exhibits a threshold of motion, controlled by the static friction coefficient and the particulate pressure, and a shear rate dependence of the particulate shear stress characteristic of a viscous like behaviour. The phenomenological laws $\mu(I)/\phi(I)$ are based on dimensional analysis where I represents the dimensionless number controlling the friction coefficient $\mu(I)$ and the volume fraction $\phi(I)$ (Forterre and Pouliquen, 2008). It can be interpreted as the ratio of a vertical time scale of rearrangement to an horizontal time scale of deformation. When the deformation time scale is large (small shear rate) compared with the time scale of rearrangement the granular media is in the quasi-static regime ($I << 1$). When the

[1] LEGI Domaine Universitaire, BP 53, 38041 Grenoble Cedex 9, France. Thibaud.revil-baudard@legi.grenoble-inp.fr
[2] LEGI Domaine Universitaire, BP 53, 38041 Grenoble Cedex 9, France. Julien.chauchat@grenoble-inp.fr

parameter I is of order unity ($I \approx 1$), the granular media is in the liquid regime of dense granular flows. In this regime, the concentration $\phi(I)$ decreases and the friction coefficient $\mu(I)$ increases with the dimensionless number I. When the parameter I is much greater than unity ($I >> 1$), the granular media is in the gaseous regime. The $\mu(I)/\phi(I)$ rheology is valid in the range $\phi \in [0.3 : 0.585]$ for spheres. In this paper, we focus on uniform steady sheet flows. The domain is split in two sub-layers : a sediment bed layer (SBL) and a fluid layer (FL) as shown in figure 1. In the SBL, the phenomenological laws $\mu(I)/\phi(I)$ are used to account for the intergranular stresses and the dilatancy effects inside the sediment bed layer. As a first step a simple mixing-length model is used to model the fluid Reynolds stresses in both FL and SBL. In the FL, the intergarnular stresses are considered negligible and a Rouse profile is assumed to represent the suspension. The main objectives of the present contribution are to propose an alternative approach to describe the intergranular stresses based on the dense granular flow rheology for the modelling of sheet flow regime and to give some clue to better understand the transition from the bottom of the sheet flow layer up to the fluid flow. To answer that, the velocity and concentration profiles predicted by the present model are compared to existing data from the literature and the evolution of the solid load is compared to experimental data for a wide range of Shields number. An investigation of the vertical structure of the sheet flow layer is then presented.

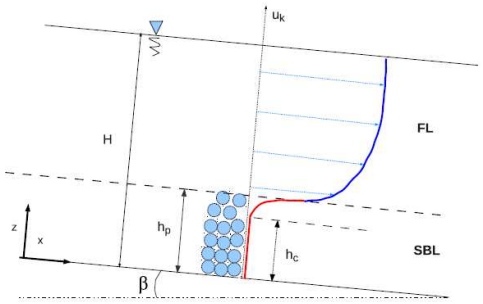

FIGURE 1 – Sketch of unidirectional sheet flow

2. Model Formulation

Horizontal and vertical momentum equations are solved for both fluid and solid phases in the SBL (equations 1-4) whereas in the FL, only the mixture is considered (5-6). In the entire domain the problem is assumed uniform and steady. In the following, u^f and u^p represent fluid and particles stream-wise velocities. ϵ and ϕ represent fluid and solid phase volume fractions and volume conservation implies $\epsilon+\phi = 1$. A mixture velocity is defined as the volume averaged velocity : $U = \epsilon u^f+\phi u^p$. σ_f et σ_p represent the fluid and particle shear stresses and P^p, P^f are particulate and fluid pressures respectively. R_{xz}^f represents the turbulent Reynolds stresses.

$$0 = \frac{\mathrm{d}\tau_{xz}^p}{\mathrm{d}z} + nf_x + \phi\,\rho_p\,g\,\sin\beta \qquad (2)$$

$$0 = -\frac{\mathrm{d}P^f}{\mathrm{d}z} - nf_z - \epsilon\rho_f g\cos\beta \qquad (3)$$

$$0 = -\frac{\mathrm{d}P^p}{\mathrm{d}z} + nf_z - \phi\rho_p g\cos\beta \qquad (4)$$

(1) (5)

$$0 = 0 = -\frac{dP^f}{dz} + \rho_f g \cos\beta \sin\beta \tag{6}$$

2.1. The fluid stresses

There are two contributions to the fluid stresses in this problem. First, the effective viscosity η_e, depending on the concentration is computed using Boyer et al. (2011) formula (8). This relationship has been set using isodense suspensions in a rheometer :

$$\tau_{xz}^f = \eta_e \frac{dU^f}{dz}. \tag{7}$$

$$\frac{\eta_e}{\eta_f} = 1 + \frac{5}{2}\phi\left(1 - \frac{\phi}{\phi^m}\right)^{-1}. \tag{8}$$

with η_f the fluid molecular viscosity and ϕ^m the maximum packing fraction. Second, the Reynolds turbulent stresses are modelled by a turbulent viscosity and a mixing length (9-10). The mixing length value depends on the integral of the concentration profile to take into account the turbulent attenuation due to the presence of particle (Li and Sawamoto, 1995). This empirical formulation allows to inhibit turbulence in the dense static bed ($\phi = \phi^m$), and leads to a classical linear Prandtl mixing length in clear water ($\phi = 0$). The computed value of the mixing length at the interface FL/SBL is used as a boundary condition for the FL resolution.

$$R_{xz}^f = \eta_t \frac{dU^f}{dz} \text{ with } \eta_t = \rho_f (1-\phi) l_m^2 \left|\frac{dU^f}{dz}\right|. \tag{9}$$

$$l_m = \kappa \int_0^z \frac{\phi^m - \phi}{\phi^m} dz. \tag{10}$$

where κ is set to 0.35.

2.2. The particles stresses

The $\mu(I)$ rheology is used to compute particulate stresses in the SBL. In this approach the shear stress is proportional to the particles pressure,

$$\tau_{xz}^p = \mu(I) P^p. \tag{11}$$

and the frictional coefficient μ evolves with the inertial number I, from a static value, μ_s, (i.e. the angle of repose of sediment) to a dynamical one, μ_2, set to 0.7 consistently with the dry granular rheology (Forterre and Pouliquen, 2008) :

$$\mu(I) = \mu_s + \frac{\mu_2 - \mu_s}{I_0/I + 1}. \tag{12}$$

where I_0 is an empirical parameter set to 0.3. The inertial number I comes from dimensional analysis of granular flows and represents the competition between the shearing of the granular media, which induces collisions and dilatancy, and the recompaction induced by the particulate pressure. For massive particles the granular flow regime is in the inertial regime (Revil-Baudard and Chauchat, 2013), and the number I reads :

$$I = \frac{\frac{du^p}{dz}}{d_p\sqrt{\frac{\rho_p}{P^p}}}. \tag{13}$$

The $\mu(I)$ rheology allows to predict the position of the lower interface of the sheet flow layer and the I dependence of the frictional coefficient expresses the increase of momentum transfer due to collisions when the granular media is highly sheared. However, it should be notice that the $\mu(I)$ rheology only applies for dense granular flows (i.e. $\phi > 0.3$).

2.3. Concentration profile

In the SBL, the Boyer et al. (2011)'s $\phi(I)$ dilatancy law is used to compute the concentration profile,

$$\phi(I) = \frac{\phi^m}{1 + b\, I^2}. \tag{14}$$

where b is an added empirical parameter set to 0.75. In the FL, a Rouse profile is assumed in the mixture and the concentration is computed from an equilibrium of the settling rate and the turbulent vertical dispersion. The reference concentration of the Rouse profile at the interface, ϕ_{hp}, is given by the dilatancy law from the SBL resolution.

$$\phi(z) = \phi_{hp} \exp\left(w_s \int_{h_p}^{z} -\frac{\rho_f}{\eta_t} \mathrm{d}z \right). \tag{15}$$

where w_s is the settling velocity of a particle.

2.4. Phases interactions

In the SBL, both phases exchange momentum in the vertical and horizontal directions. On the vertical direction, the weight of the displaced fluid gives rise to the buoyancy force on the particulate phase,

$$n f_z = -\phi \frac{\mathrm{d}P^f}{\mathrm{d}z}. \tag{16}$$

In the horizontal direction, the generalised buoyancy represents the effect of the local shearing of the fluid phase or equivalently the effect of its acceleration (Jackson, 2000). This term can be seen as the part of the fluid viscous shear stresses which apply on particles. Indeed, it is assumed that the viscous shear stresses apply on both phases and that each contribution is weighted by their respective local volume fraction. On the opposite, the intergranular stresses only apply on the particulate phase without transferring momentum to the fluid one. The second contribution, related to the relative velocity between fluid and particulate phases, corresponds to the drag force :

$$n f_x = \phi \frac{\mathrm{d}\tau_{xz}^f}{\mathrm{d}z} + C_D\,(U^f - u^p). \tag{17}$$

Following Jenkins and Hanes (1998) and Hsu et al. (2004), the Dallavalle formulae (18) is used with Richardson and Zaki (1954)'s correction for the drag coefficient :

$$C_D = \frac{\rho_f \phi}{d_p\,(1-\phi)^{2.1}} \left(0.3\,(U^f - u^p) + 18.3\, \frac{\eta_f}{\rho_f\, d_p} \right). \tag{18}$$

2.5. Model equations

Finally, the proposed model can be summarised as follow in the SBL :

$$0 = \frac{\mathrm{d}R_{xz}^{f}}{\mathrm{d}z} + \varepsilon \frac{\mathrm{d}\tau_{xz}^{f}}{\mathrm{d}z} - C_D\,(U^f - u^p) + \varepsilon\,\rho_f\,g\,\sin\beta. \tag{19}$$

$$0 = \frac{\mathrm{d}\tau_{xz}^{p}}{\mathrm{d}z} + \phi \frac{\mathrm{d}\tau_{xz}^{f}}{\mathrm{d}z} + C_D\,(U^f - u^p) + \phi\,\rho_p\,g\,\sin\beta. \tag{20}$$

$$\frac{\mathrm{d}P^f}{\mathrm{d}z} = \rho_f g \cos\beta \quad \text{and} \quad \frac{\mathrm{d}P^p}{\mathrm{d}z} = \phi\Delta\rho g \cos\beta. \tag{21}$$

and in the FL :

$$\frac{\mathrm{d}P^f}{\mathrm{d}z} = \rho_f g \cos\beta \quad \text{and} \quad 0 = \frac{\mathrm{d}\tau_{xz}^{f}}{\mathrm{d}z} + \frac{\mathrm{d}R_{xz}^{f}}{\mathrm{d}z} + \rho_f\,g\,\sin\beta. \tag{22}$$

These equations are discretised and solved in a semi-implicit scheme using finite difference. This two-layer model allows to separate flow regimes. In the FL, a fluid-dominant mixture is considered and the suspended particles are assumed quasi-passive : they do not take part to particulate pressure, and weakly affect turbulent viscosity (equation 10). However, in the SBL both phases diffuse momentum and interact. In the FL, the mixture flows because of the slope and applies a shear stress which set in motion the sediment bed layer (also affected by gravity). The SBL resolution gives back the interface velocity and the turbulent characteristics as boundary conditions for the FL resolution. This scheme is then repeated to reach an equilibrium state (Revil-Baudard and Chauchat, 2013)

3. Results and discussion

The present model has been used to simulate sheet flows of massive particles. The sediment properties come from Sumer et al. (1996)'s experiments and are presented in table 1. First, velocity and concentration profiles for runs 82, 91, 99 of Sumer et al. (1996) are presented and the present model results are compared to other data from literature. Second, the predicted solid load depending on the Shields number is compared to data from literature and the vertical profile of sediment flux for the run 91 is discussed. Third, the different mechanisms acting in the sheet flow regime are analysed. Finally the feedback of the mobile bed on the fluid layer is investigated through the equivalent roughness.

3.1. Velocity and concentration profiles

The model has been validated against Sumer et al. (1996)'s experiments (runs 82, 91, 99) involving massive plastic particles (table 1). The experimental conditions for each run are presented in table 2. Figure 2(a) shows the comparison between the present model results and the measurements for velocity profiles. A good agreement is observed between simulated and measured velocity profiles, especially in the sediment bed layer where the $\mu(I)$ rheology predicts a smooth decrease of the velocity toward the static bed. The very low relative velocity between fluid and sediment in the SBL is explained by the large size of particles which induces an important drag force. The differences observed between measured and computed velocities in the upper part of the fluid layer can be due to different reasons : the absence of an outer layer modelling, the presence of 3D effects and/or the rather crude modelling of the lid at the channel surface. A more refined turbulence model is required to improve the two-phase model results, however it is beyond the scope of the present study. Figure 2(b) shows the concentration profiles obtained with the present frictional model compared with the ones obtained using the kinetic theory of granular flows from

Hsu et al. (2004). Both approaches predict a zone of constant concentration characteristic of a sheet layer. It is also observed that the thickness of this concentration "shoulder" increases with the Shields number. It should be noticed that the concentration in the SBL is always larger than 0.3 which correspond to the validity domain of the $\mu(I)/\phi(I)$ laws. These comparisons demonstrate the relevancy of this phenomenological approach to describe intense bed-load transport (sheet flow) and validate this model for different flow conditions.

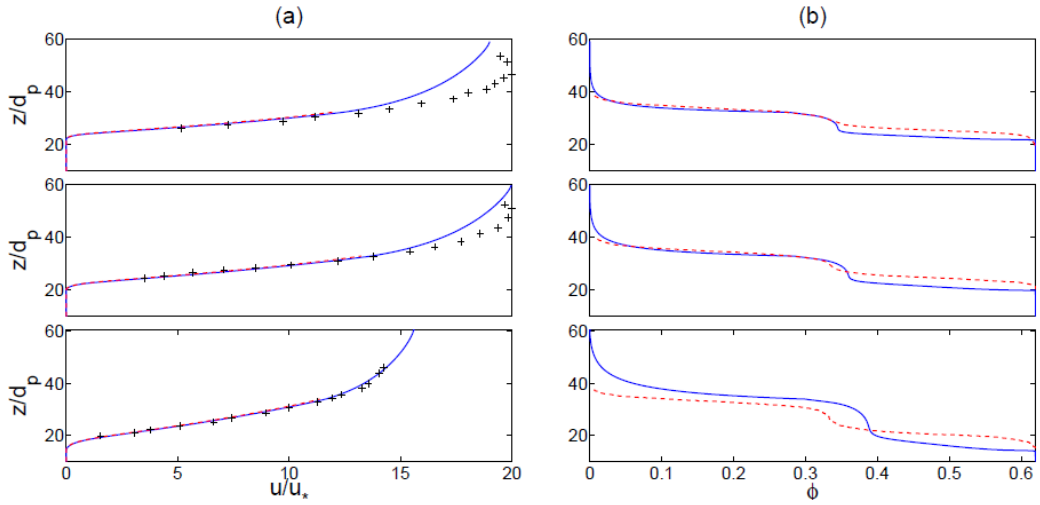

FIGURE 2 – Comparison of the fluid (—) and the particulate (- - -) velocity profiles between the present model and the measurements of Sumer et al. (1996) (+) in (a). The concentration profiles predicted by the present model (—) are compared with Hsu et al. (2004)'s results (- - -) and are shown in (b). From top to bottom the left and right panels correspond to Run 82 (θ = *1.37*), Run 91 (θ = *1.65*) and Run 99 (θ = *2.3*) of Sumer et al. (1996)'s experiments.

TABLE 1 – Sediment properties.

Composition	Shape	d_p (mm)	ρ_p (kg.m^{-3})	ϕ^m	μ_s	μ_2	w_s (m/s)
PMMA	Cylinders	2.6	1140	0.62	0.51	0.7	0.072

TABLE 2 – Run conditions

Sumer et al. **(**1996**)'s run number**	θ	u_* (m/s)	*sin* β	H_p (cm)	h_p (cm)	ρ_f (kg.m^{-3})	η_f (kg. m^{-1}. s^{-1})	κ
82	1.37	0.1	0.00715	17.4	*8.4*	10^3	10^{-3}	0.35
91	1.64	0.11	0.0086	17.5	*8.5*	10^3	10^{-3}	0.35
99	2.30	0.125	0.0119	17.6	*8.8*	10^3	10^{-3}	0.35

3.2. Solid load and sediment flux profiles

Simulations of sheet flow regimes over a wide range of Shields number ($0.5 < \theta < 2.5$) and with the same sediment particles have been performed. The total solid load per unit width (in the SBL and in the FL) and the bed-load contribution, defined as the solid load in the SBL, are compared with experimental data as summarised by Yalin (1977) (figure 3). A power law fit of the dimensionless total solid load versus the Shields number is presented in the inset of figure 3. The good agreement with experiments obtained for the solid load over a wide range of shields number together with the power law evolution confirm the good behaviour of the model. The comparison between suspended load and bed load shows that the bed-load is dominant which is consistent with Sumer et al. (1996)'s phase diagram in the plane $[\theta, w_s/u_*]$ that allows to differentiate suspension and no-suspension modes for sheet-flow regime. In the present simulations, the ratio of the settling velocity over the frictional one is in the range $w_s/u_* \in [0.74;1.7]$, which mainly corresponds to the "no-suspension mode".

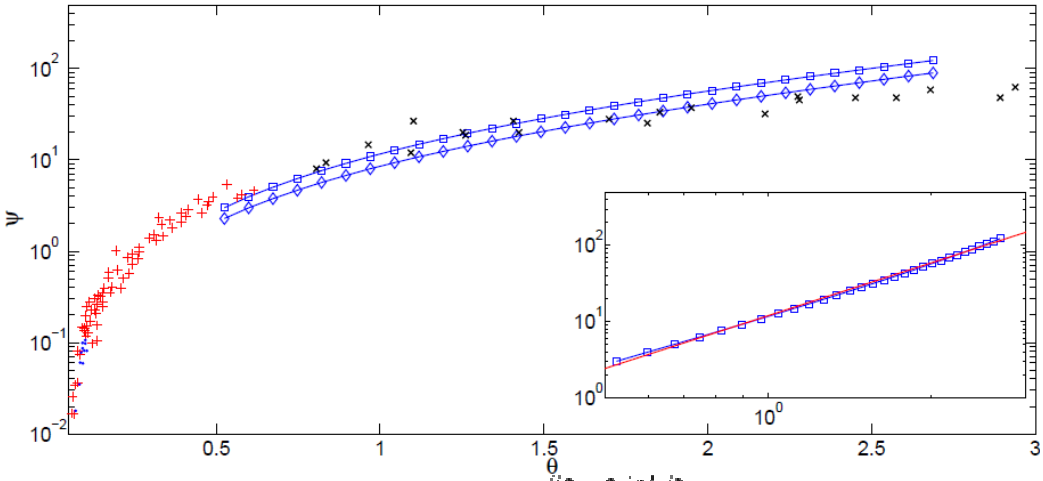

FIGURE 3 – Solid load per unit width scaled by $d_p\sqrt{(s-1)gd_p}\rho_f$ with respect to the Shields parameter θ. Experimental data from Meyer-Peter and Muller (1948) (+), Wilson (1966) (x), Gilbert (1914) (·) synthesized in Yalin (1977) ; total load and bed load results from the present model(□,◇). The best fit of the model result, $\psi = 11.9\,\theta^{2.3}$ (—) is represented in log-log scales in the inset.

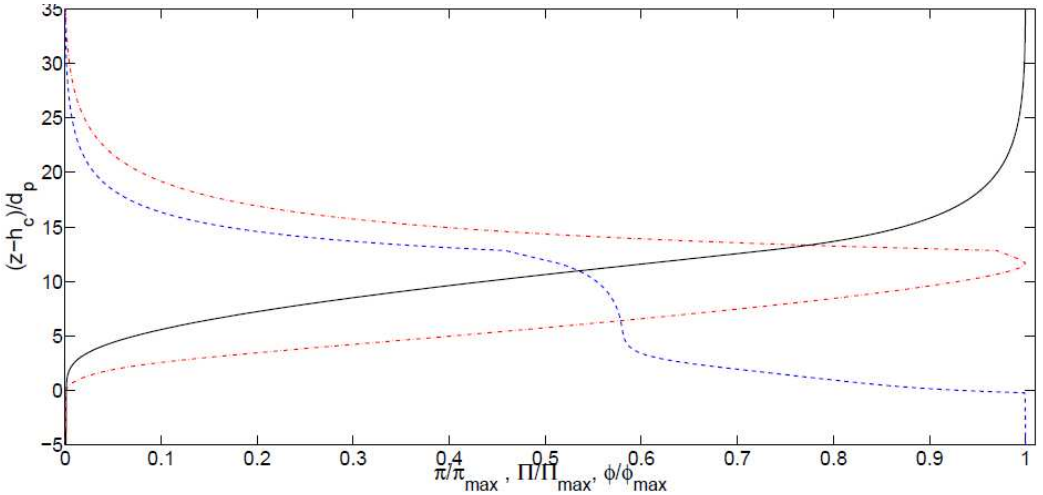

FIGURE 4 – Concentration - - -, sediment flux - . - and cumulated sediment flux — for Sumer et al. (1996)'s experiment, run 91 ($\theta = 1.64$) with $w_s/u_* = 0.94$

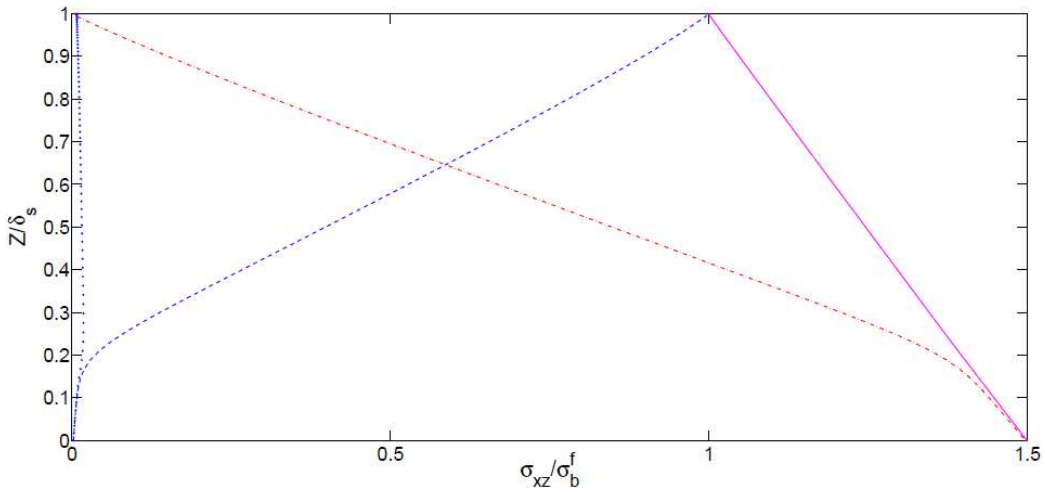

FIGURE 5 – Results of the various contributions to the total mixture stresses inside the SBL, non-dimensionalised by the shear stress at the interface SBL/FL (σ_b^f), for run 91 of Sumer et al. (1996). The vertical axis starts at the lower limit of the sheet and is non-dimensionalised by the thickness. — represents the mixture stresses, - . - represents the particulate stresses, - - - represents the total fluid stresses and . . . represents the viscous contribution to fluid stresses.

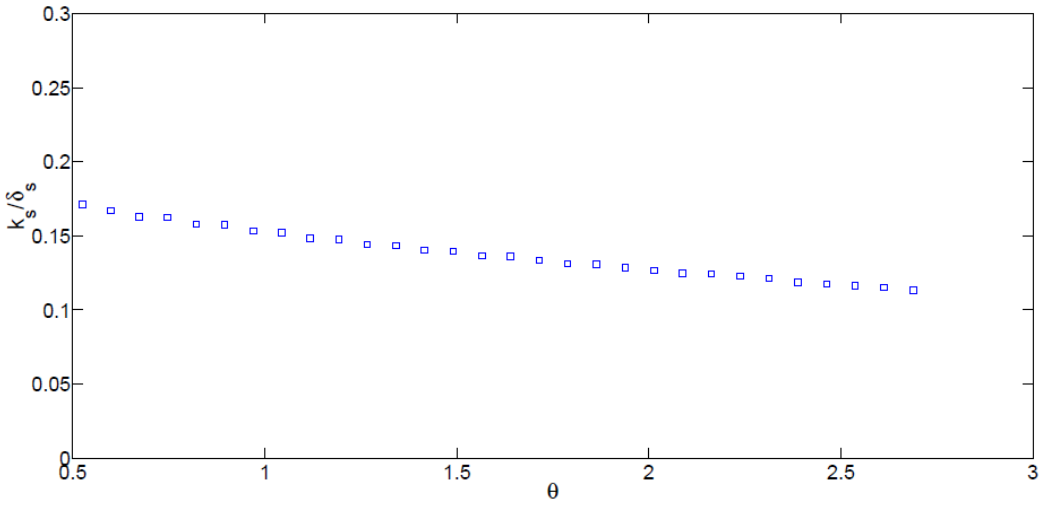

FIGURE 6 – Roughness k_s scaled by the thickness δ_s with respect to the Shields parameter θ.

In order to determine the preferential regions of sediment flux, the concentration, the flux ($\pi = \phi \times u^p$) and the cumulative flux ($\Pi(z)$ integral from 0 to z of the flux) profiles associated to run 91 are presented in figure 4. It is shown that the maximum flux is located at the top of the concentration shoulder, close to the FL/SBL interface. The curve of cumulative flux shows that about 75% of the total load pertains to the sheet layer. This result argues for the importance of a better understanding of the sheet flow regime for large scale morphodynamic studies, particularly in the case of massive particles.

3.3. Discussion

In order to investigate the relative contribution of intergranular, viscous and turbulent stresses in the SBL the different contributions to the total shear stresses are presented in figure 5. First, it is interesting to note that the viscous contribution is negligible over the entire sheet layer. Second, three layers can be distinguished in the sheet flow layer : i) A granular dominated layer, close to the lower interface of the

sheet flow layer, where the frictional stresses dominate and control the sheet layer thickness ; ii) A layer where both intergranular and fluid stresses are of the same order of magnitude, corresponding to the concentration shoulder region ; iii) Finally, in the upper layer, the intergranular stresses vanish and the total stresses are dominated by the turbulent ones. It is interesting to note that the zone of maximum flux (figure 5) is close to the upper interface of the mobile bed where the shear stresses is dominated by the turbulent ones. This result confirms that turbulence modelling at the transition from the dense mobile bed layer to the suspension is the key issue for two-phase modelling of sheet-flow regime. The use of the $\mu(I)$ rheology allows to capture the transition from the mobile bed layer to the fixed bed however the sediment flux in this layer is small. This probably explains why models that did not describe this transition accurately are able to obtain good predictions of solid load.

It has been observed experimentally that the equivalent roughness increases as the Shields number and the solid load increase (Nnadi and Wilson, 1992; Sumer et al., 1996). Therefore, the fluid motion above the mobile bed is affected by the sheet flow layer. Figure 6 shows the evolution of the equivalent roughness, defined as the value of the mixing length at the top of the interface non-dimensionalised by the sheet flow layer thickness, with respect to the Shields number. It should be noticed that the dimensionless roughness is rather constant over the whole range of investigated Shields numbers. This result confirms that the relevant length scale for the roughness is the mobile bed layer thickness rather than the particle size. A possible interpretation of this roughness increase with the sheet-flow layer thickness can be attributed to the penetration of turbulence structures in the upper layer of the sheet. These structures tend to dissipate the flow energy, like an increase of the geometrical roughness would do. The choice of a mixing length parameterised by the integral of the solid volume fraction allows to link the turbulent length scale to the mobile bed layer thickness. These hypotheses have to be further investigated through more refined numerical models and small scale laboratory experiments.

4. Conclusion

The use of a dense frictional rheology and a simple mixing length approach in a two-phase model is shown to be sufficient for the prediction of the main features of the sheet flow regime. The present results demonstrate that the dense granular flow rheology $\mu(I)$ together with the dilatancy law $\phi(I)$ are relevant to describe the transition from the fixed bed to the mobile bed layer. Our results also confirm that turbulent processes in the upper layer of the sheet flow are the key issue for solid load predictions and that the sheet flow layer thickness is the relevant length scale for turbulence modelling. Laboratory experiments are required to better understand small scale turbulent processes in sheet flow conditions.

Acknowledgements
The authors would like to acknowledge DGA for the financial support of the first author PhD Thesis (N° 2011-170914/DGA/DS/MRIS)

Références

Bagnold, R. A. 1954, Experiments on a gravity-free dispersion of large solid spheres in a newtonian fluid under shear, *Phil. Trans. R. Soc. Lond.*, *225*, 49–63.

Boyer, F. m. c., E. Guazzelli, and O. Pouliquen 2011, Unifying suspension and granular rheology, *Phys. Rev. Lett.*, *107*, 188,301, doi :10.1103/PhysRevLett.107.188301.

Cassar, C., M. Nicolas, and O. Pouliquen 2005, Submarine granular flows down inclined planes, *Physics of Fluids*, *17*(10), 103301, doi :10.1063/1.2069864.

Forterre, Y., and O. Pouliquen 2008, Flows of dense granular media, *Annual Review of Fluid Mechanics*, *40*, 1–24, doi :10.1146/annurev.fluid.40.111406.102142.

GDR midi 2004, On dense granular flows, *The European Physical Journal E*, *14*, 341–365.

Gilbert, G. K. 1914, The transportation of debris by running water, *Tech. Rep. 86*, USGS Professional Paper.

Hanes, D. M., and A. J. Bowen 1985, A granular-fluid model for steady intense bed-load transport, *J. Geophys. Res., Vol. 90*.

Hsu, T.-J., J. T. Jenkins, and P. L.-F. Liu 2004, On two-phase sediment transport : sheet flow of massive particles, *Proceedings of the Royal Society of London. Series A : Mathematical, Physical and Engineering Sciences*, (*460*2048), 2223–2250, doi :10.1098/rspa.2003.1273.
Jackson, R. 2000, *The dynamics of fluidized particles*, Cambridge University Press, Cambridge.
Jenkins, J. T., and D. M. Hanes 1998, Collisional sheet flows of sediment driven by a turbulent fluid, *Journal of Fluid Mechanics*, *370*-(1), 29–52.
Li, and Sawamoto 1995, Multi-phase model on sediment transport in sheet-flow regime under oscillatory flow, *Coastal engineering Japan*, *38*, 157–178.
Meyer-Peter, E., and R. Muller 1948, Formulas for bed-load transport, in *2nd Meeting of the International Association of Hydraulic and Structural Research*, pp. 34–64.
Nnadi, F. N., and K. C. Wilson 1992, Motion of contact-load particles at high shear stress, *Journal of Hydraulic Engineering*, *118*(12), 1670–1684, doi :10.1061/(ASCE)0733-9429(1992)118 :12(1670).
Revil-Baudard, T., and J. Chauchat 2013, A two-phase model for sheet flow regime based on dense granular flow rheology, *Journal of Geophysical Research*, doi :doi :10.1029/2012JC008306, in press.
Richardson, J. F., and W. N. Zaki 1954, Sedimentation and fluidization : Part i, *Trans. Instn. Chem. Engrs*, *32*.
Sumer, B. M., A. Kozakiewicz, J. F. e, and R. Deigaard 1996, Velocity and concentration profiles in sheet-flow layer of movable bed, *Journal of Hydraulic Engineering*, *122*(10), 549–558, doi :10.1061/(ASCE)0733-9429(1996)122 :10(549).
Wilson, K. 1987, Analysis of bed-load motion at high shear stress, *Journal of Hydraulic Engineering*, *113*, 97–103.
Wilson, K. C. 1966, Bed-load transport at high shear stress, in *Proc. A.S.C.E*, vol. HY6, ASCE.
Yalin, M. S. 1977, *Mechanics of sediment transport 2nd edition*, Pergamon Press, Ontario.